

Cortical thickness in Parkinson's disease: a coordinate-based meta-analysis

LiQin Sheng¹, PanWen Zhao², HaiRong Ma¹, Joaquim Radua^{3,4,5}, ZhongQuan Yi², YuanYuan Shi², JianGuo Zhong^{6,*}, ZhenYu Dai^{7,*}, PingLei Pan^{6,*}

¹Department of Neurology, Kunshan Hospital of Traditional Chinese Medicine, Kunshan, PR China

²Department of Central Laboratory, The Yancheng School of Clinical Medicine of Nanjing Medical University, Yancheng, PR China

³Imaging of Mood- and Anxiety-Related Disorders (IMARD) Group, Institut d'Investigacions Biomèdiques August Pi i Sunyer (IDIBAPS), CIBERSAM, Barcelona, Spain

⁴Early Psychosis: Interventions and Clinical-Detection (EPIC) Laboratory, Department of Psychosis Studies, Institute of Psychiatry, Psychology and Neuroscience, King's College London, London, UK

⁵Centre for Psychiatric Research and Education, Department of Clinical Neuroscience, Karolinska Institutet, Stockholm, Sweden

⁶Department of Neurology, The Yancheng School of Clinical Medicine of Nanjing Medical University, Yancheng, PR China

⁷Department of Radiology, The Yancheng School of Clinical Medicine of Nanjing Medical University, Yancheng, PR China

*Equal contribution

Correspondence to: PingLei Pan; **email:** plpan@njmu.edu.cn

Keywords: Parkinson's disease, cortical thickness, surface-based morphometry, coordinate-based meta-analysis, seed-based *d* mapping

Received: September 10, 2020 **Accepted:** November 30, 2020 **Published:** January 10, 2021

Copyright: © 2021 Sheng et al. This is an open access article distributed under the terms of the [Creative Commons Attribution License](https://creativecommons.org/licenses/by/3.0/) (CC BY 3.0), which permits unrestricted use, distribution, and reproduction in any medium, provided the original author and source are credited.

ABSTRACT

Parkinson's disease (PD) is a common age-related neurodegenerative disease that affects the structural architecture of the cerebral cortex. Cortical thickness (CTH) via surface-based morphometry (SBM) analysis is a popular measure to assess brain structural alterations in the gray matter in PD. However, the results of CTh analysis in PD lack consistency and have not been systematically reviewed. We conducted a comprehensive coordinate-based meta-analysis (CBMA) of 38 CTh studies (57 comparison datasets) in 1,843 patients with PD using the latest seed-based *d* mapping software. Compared with 1,172 healthy controls, no significantly consistent CTh alterations were found in patients with PD, suggesting CTh as an unreliable neuroimaging marker for PD. The lack of consistent CTh alterations in PD could be ascribed to the heterogeneity in clinical populations, variations in imaging methods, and underpowered small sample sizes. These results highlight the need to control for potential confounding factors to produce robust and reproducible CTh results in PD.

INTRODUCTION

Parkinson's disease (PD), the second most common neurodegenerative disease after Alzheimer's disease,

affects 6.1 million individuals worldwide. The incidence of PD increases rapidly with age making it a major source of disability and global health burden [1–3]. PD is a highly clinically heterogeneous condition

that is characterized by both cardinal motor symptoms, such as resting tremor, rigidity, and bradykinesia, and several non-motor symptoms throughout disease course, such as cognitive impairment, apathy, depression, anxiety, impulse control disorders, sleep disturbance, fatigue, pain, visual hallucinations, and autonomic dysfunction [4, 5]. The pathophysiology of PD is complex and involves several neural networks in addition to dopaminergic dysfunction [6–9]. Neurodegeneration may occur several years before PD is diagnosed based on characteristic motor symptoms [10]. Modern neuroimaging techniques have immensely contributed to the understanding of pathophysiology, early and differential diagnosis, severity, and progression of PD [6, 9, 11, 12].

Although degeneration of the substantia nigra is the primary histopathological feature of PD, the cerebral cortex is also affected as the disease progresses [13]. Cortical thickness (CTh) analysis of structural magnetic resonance imaging (MRI) data is a highly validated and popular surface-based technique for assessing changes in cortical gray matter (GM). Compared to voxel-based morphometry (VBM) that measures the regional GM volume as the product of the cortical surface area, CTh, and/or cortical folding, CTh analysis is more sensitive and directly assesses cortical morphology [14–17]. CTh analysis has been widely used to assess brain morphology in PD in relation to demographic and clinical characteristics, such as the age of onset, age, disease duration, motor deficits, disease stages, and divergent non-motor symptoms [17–43]. Certain study groups reported that CTh alterations served as indicators of neural degeneration in PD [15, 44], whereas others failed to identify cortical morphological features in patients with PD as compared with healthy controls (HCs) [38, 45–49]. Despite significant advances in understanding the neurobiological characteristics of PD, CTh analysis results lack consistency and have not been systematically reviewed.

A coordinate-based meta-analysis (CBMA) quantitatively combines data from individual neuroimaging studies to assess brain regions with significantly consistent structural or functional alterations in a particular neuropsychiatric disorder using the location of peak coordinates in three-dimensional (3D) anatomical spaces (x, y, z) [50, 51]. Recently, CBMA has been developed for surface-based morphometry (SBM) studies to identify consistent CTh abnormalities in major depressive disorder [52]. We conducted a CBMA of SBM studies to investigate CTh alterations in PD using seed-based *d* mapping with the permutation of subject images (SDM-PSI) [53, 54] and following the recent guidelines and recommendations [50, 51].

RESULTS

Included studies and characteristics

A literature search produced 602 results, of which 38 studies finally met the inclusion criteria [15, 17, 20, 22, 24, 25, 31, 33–39, 41, 43–49, 55–70]. The flowchart in Figure 1 shows the study selection process. These studies included 57 PD-HC comparison datasets comprising 1,843 non-demented patients with PD (mean age: 62.87 years) and 1,172 HC subjects (mean age: 62.48 years). Sample sizes in the included datasets ranged from 8 to 151 (mean: 32.33) in the patient group and from 10 to 58 (mean: 29.3) in the HC group. The following demographic and clinical characteristics were reported in these studies: gender distribution in 53 datasets (56.32% male in the patient group and 54.48% male in the HC group), education level in 35 datasets (mean of 12.21 years in the patient group and a mean of 12.98 years in the HC group), disease duration in 54 datasets (mean: 5.43 years), Hoehn and Yahr (HY) stage in 45 datasets (mean: 2.05), United Parkinson's disease rating scale, part III (UPDRS-III) in 52 datasets (mean: 23.62 without considering the medication state), levodopa equivalent daily dose (LEDD) in 35 datasets (mean: 506.33mg), and mini-mental state examination (MMSE) in 37 datasets (mean of 26.98 in the patient group and a mean of 28.68 in the HC group) (Supplementary Table 2). As listed in Supplementary Table 3, 3.0 Tesla MRI scanners were applied to 46 datasets (80.7%), and 50 datasets (87.7%) used thresholds corrected for multiple comparisons in the statistical analysis. Of the 57 datasets, only 26 (45.6%) underwent quality control for imaging data by a visual check and/or a subsequent manual edit as mentioned in the articles. Quality assessment scores of the included studies are listed in Supplementary Table 2.

Main CBMA

We detected no consistent CTh differences between patients with PD and HC subjects ($n = 57$ datasets) using the threshold-free cluster enhancement (TFCE)-based family-wise error (FWE) correction ($p < 0.05$ and voxel extent ≥ 10). Although we used a less stringent significance level (uncorrected $p < 0.005$ and voxel extent ≥ 10), there was still a lack of significant results.

Subgroup CBMA

The following datasets were used to conduct eight subgroup CBMAs: datasets obtained using 3.0 Tesla MRI scanners ($n = 46$), datasets with a slice thickness of lower than 1 mm or voxel size lower than $1 \times 1 \times 1$ mm³ ($n = 48$), datasets processed using FreeSurfer software

packages ($n = 51$), datasets with full width half 15 mm or less ($n = 44$), datasets with at least one covariate included in the statistical model ($n = 42$), and datasets for which thresholds were corrected for multiple comparisons ($n = 50$), datasets with quality

maximum (FWHM) of the smoothing kernel size of control of imaging data ($n = 26$), and those not specifying it ($n = 31$). None of the subgroup CBMAs demonstrated significantly consistent findings using the TFCE-based FWE correction ($p < 0.05$ and voxel extent

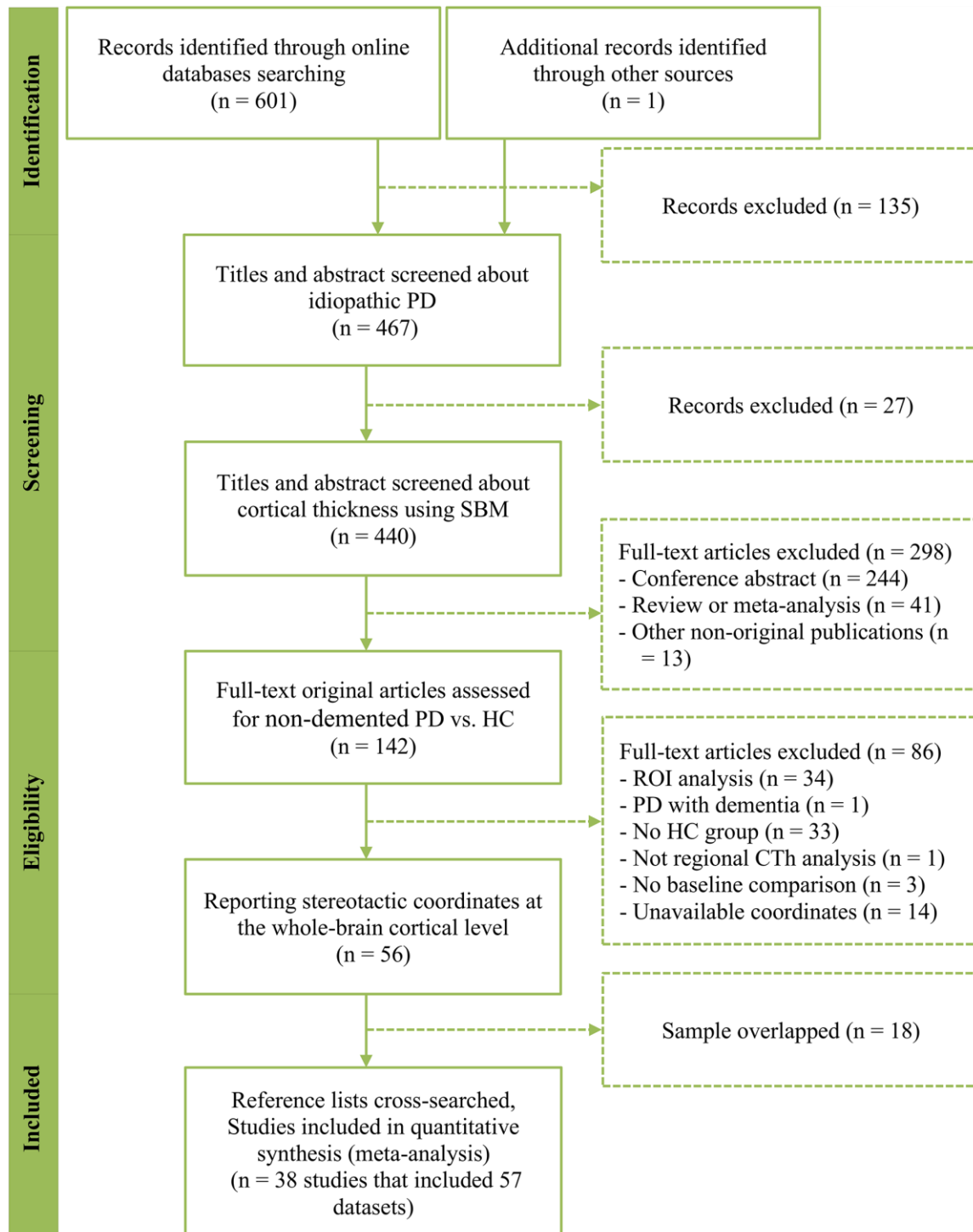


Figure 1. PRISMA flow chart describing the study selection process. PRISMA, Preferred Reporting Items of Systematic Review and Meta-Analysis; PD, Parkinson’s disease; SBM, surface-based morphometry; CTh, cortical thickness; ROI, region of interest.

≥ 10). Other subgroup CBMAs were not conducted because of the insufficient datasets included. Of the datasets included, only a few datasets explicitly subtyped PD patients with mild cognitive impairment (MCI) ($n = 6$). Other clinical subtypes were the case as well.

Jackknife sensitivity, heterogeneity and publication bias analyses

Jackknife sensitivity analysis revealed that the lack of significantly consistent CTh differences between patients with PD and HC subjects survived in all combination of the datasets.

We could not perform subsequent heterogeneity and publication bias analyses because the main CBMA did not reveal any significant brain clusters.

Meta-regression analysis

Meta-regression analysis revealed that a longer disease duration (available datasets $n = 54$) was associated with lower CTh in the supplementary motor area/cingulate cortex (Montreal Neurological Institute [MNI] coordinates: $x = -4$, $y = -2$, $z = 46$; Brodmann area [BA] 24; SDM-Z = -2.31 ; TFCE-based FWE corrected $p = 0.009$; voxels = 392, Figure 2A). In addition, a lower MMSE score in the PD sample (available datasets $n = 37$) was associated with lower CTh in the right superior temporal gyrus/rolandic operculum (MNI coordinates: $x = 54$, $y = -22$, $z = 12$; BAs 48 and 22; SDM-Z = 7.05 ; TFCE-based FWE corrected $p = 0.001$; voxels = 999), left superior/middle temporal gyri (MNI coordinates: $x = -62$, $y = -12$, $z = 0$; BAs 48, 21, and 22; SDM-Z = 6.65 ; TFCE-based FWE corrected $p = 0.009$; voxels = 441), and left inferior temporal gyrus (MNI coordinates: $x = -60$, $y = -20$, $z = -24$; BAs 20 and 21; SDM-Z = 6.57 ; TFCE-based FWE corrected $p = 0.03$; voxels = 169) (Figure 2B). A higher LEDD (available datasets $n = 35$) in the PD sample was associated with lower CTh in the medial prefrontal cortex/anterior cingulate cortex (MNI coordinates: $x = 4$, $y = 32$, $z = 38$; BAs 32, 24, 10, and 8; SDM-Z = -1.66 ; TFCE-based FWE corrected $p = 0.029$; voxels = 1441, Figure 2C). Other variables, such as mean age (available from all datasets), male percentage in the patient sample (available datasets $n = 53$), education level (available datasets $n = 35$), UPDRS-III (available datasets $n = 52$), and HY stage (available datasets $n = 45$) did not correlate with regional CTh alterations ($p < 0.05$ TFCE-based FWE corrected and cluster size ≥ 10 voxels). Results from meta-regression of UPDRS-III scores should be interpreted with caution as the medication state (on or off) was not stated in certain datasets included during the assessment of this score.

DISCUSSION

We conducted CBMAs of SBM studies (57 datasets) to quantitatively identify consistent CTh alterations in a large pooled sample of PD patients using the latest algorithms of SDM-PSI [53, 54] and following the recent guidelines and recommendations [50, 51]. Compared with 1,172 HC subjects, we did not detect consistent CTh alterations in 1,843 patients with PD either using a TFCE-based FWE corrected or a more lenient uncorrected threshold. Furthermore, jackknife analyses and subgroup CBMAs confirmed the non-reproducibility of results. This finding is in line with the related literature that reports a widespread lack of replicability in neuroimaging [71]. Thus, CTh analysis is an unreliable neuroimaging marker in PD.

PD is a progressive neurodegenerative disorder. It has been suggested that cortical neurodegeneration begins from stage 4 (associated with early phase motor dysfunction) according to the well-established brain pathologic staging scheme for PD proposed by Braak et al. [13]. All datasets included in the current CBMA enrolled patients with PD at their symptomatic stages, i.e., showing cortical neurodegeneration that probably manifested CTh alterations, although it is still unclear whether such alterations are a direct cause of neurodegeneration or a by-product [22]. However, our CBMA did not detect consistence of CTh alterations in PD across studies. A lack of consistent CTh abnormalities in patients with PD relative to HCs may suggest that CTh analysis of MRI data may not have the power to detect such abnormalities paralleling with the neurodegeneration. Measuring the 1–5 mm thick cortex based on (usually) 1 mm³ voxels from MRI data is made inherently challenging; however, FreeSurfer, one of the most prominent packages for automatically estimating the brain CTh, showed good agreement with histologic measurements of CTh [72]. In addition, multiple validation studies presented good comparability for detecting CTh between advanced image processing algorithms [73]. Although reports on comparisons between histology and automated techniques from *in vivo* MRI data measuring CTh alterations in PD are lacking, we attribute the presence of inconsistent CTh abnormalities in PD to heterogeneous clinical populations, variations in imaging methods, and underpowered small sample sizes.

PD is a heterogeneous disorder in terms of clinical phenotypes (motor subtypes and variable non-motor symptoms throughout the disease course) [4, 5, 74, 75] and pathogenetic features [76, 77]. As listed in Supplementary Table 2, there were variations regarding demographic and clinical characteristics across studies. Our meta-regression analyses revealed global cognitive

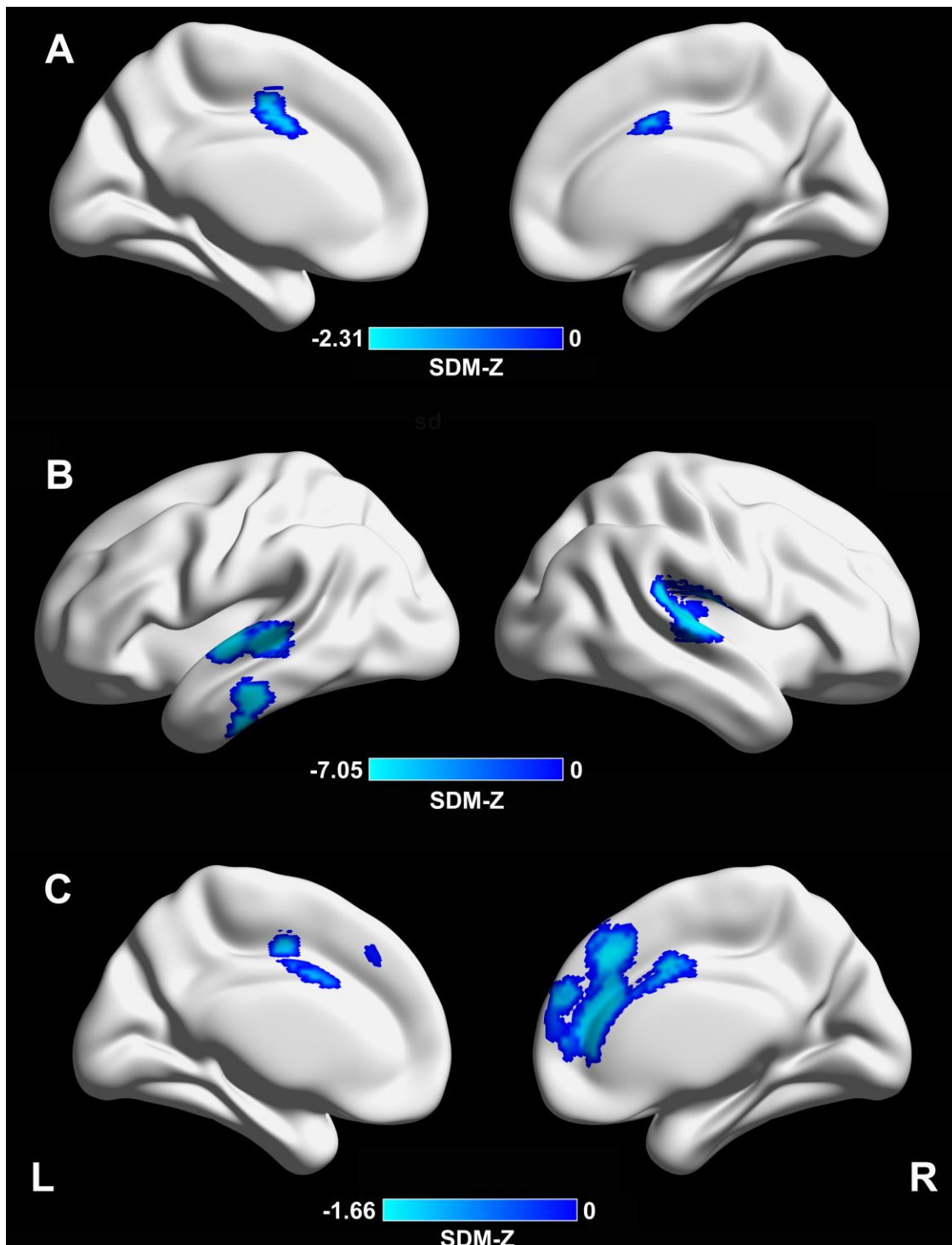


Figure 2. Meta-regression analyses of clinical variables with cortical thickness. (A) A longer disease duration was associated with lower CTh in the supplementary motor area/cingulate cortex (MNI coordinates: $x = -4$, $y = -2$, $z = 46$; BA 24; SDM-Z = -2.31 ; TFCE-based FWE corrected $p = 0.009$; voxels = 392). (B) A lower MMSE score in the PD sample was associated with lower CTh in the right superior temporal gyrus/rolandic operculum (MNI coordinates: $x = 54$, $y = -22$, $z = 12$; BAs 48 and 22; SDM-Z = 7.05 ; TFCE-based FWE corrected $p = 0.001$; voxels = 999), left superior/middle temporal gyri (MNI coordinates: $x = -62$, $y = -12$, $z = 0$; BAs 48, 21, and 22; SDM-Z = 6.65 ; TFCE-based FWE corrected $p = 0.009$; voxels = 441), and left inferior temporal gyrus (MNI coordinates: $x = -60$, $y = -20$, $z = -24$; BAs 20 and 21; SDM-Z = 6.57 ; TFCE-based FWE corrected $p = 0.03$; voxels = 169). (C) A higher LEDD in the PD sample was associated with lower CTh in the medial prefrontal cortex/anterior cingulate cortex (MNI coordinates: $x = 4$, $y = 32$, $z = 38$; BAs 32, 24, 10, and 8; SDM-Z = -1.66 ; TFCE-based FWE corrected $p = 0.029$; voxels = 1441). CTh, cortical thickness; MNI, Montreal Neurological Institute; BA, Brodmann area; SDM, seed-based d mapping; TFCE, threshold-free cluster enhancement; FWE, family-wise error; PD, Parkinson's disease; LEDD, levodopa equivalent daily dose.

function, disease duration, and LEDD as confounding factors affecting CTh alterations in PD across studies. Other variables, such as age, male gender, education level, the severity of motor disability, and disease stage did correlate with regional CTh alterations. However, these results should be interpreted with caution because analyses were conducted at the study level not at an individual subject level. In individual SBM studies, different and inconsistent patterns of CTh abnormalities have been associated with demographic and clinical characteristics, such as the age of onset [18], age [19], disease duration [19–23], gender [24], the severity of motor deficits [20, 21, 25], motor laterality [26], and disease stages [20, 25, 27]. In addition, CTh abnormalities have been reported to correlate with several non-motor symptoms, such as cognitive deficits [17, 20, 23, 28–34], impulse control disorders [35, 36], depression [37–39], progressive olfactory loss [40], rapid eye movement sleep behavior disorder [41], pain [42], and mild behavioral impairment [43]. Furthermore, different subtypes of MCI in PD (amnesic MCI and non-amnesic MCI, MCI reverters and MCI non-reverters) demonstrate distinct patterns of CTh alterations [34, 58, 78]. Moreover, brain-derived neurotrophic factor (BDNF) Val66Met polymorphism in PD affects cortical thinning pattern [79]. Using a hypothesis-free, CTh data-driven approach, Uribe et al. identified three cortical phenotypes affected in non-demented PD patients [80], with different progressive patterns over time [81] that may detect prognosis markers in PD [80, 81]. Although several longitudinal studies showed that CTh alterations in PD were sensitive to time [44, 79, 81, 82], the majority of previous studies did not comprehensively distinguish PD subtypes and conducted neuroimaging analyses only at one time point. Thus, heterogeneity in clinical populations resulted in inconsistencies and a lack of reproducibility across CTh studies. Well-characterized subtype-homogeneous samples with both cross-sectional and longitudinal designs can improve the reproducibility [51].

Apart from the heterogeneity in clinical populations, inconsistent CTh alterations in PD are attributed to variations in imaging methods. As shown in Supplementary Table 3, we noted variations in scanner manufacturer and platform, field strength, head coil, MR sequence, and voxel size. MRI data of most SBM studies included in the CMBA were acquired at a single site except for the Parkinson's Progression Markers Initiative (PPMI) cohort, a multicenter database [68]. Several studies have reported the effects of scanner platform [83, 84], field strength [85–87], pulse sequence [85, 88, 89], number of coil channels [88], scanner relocation [90], imaging sites [83, 91], type of computing workstation [92], and operating systems [92,

93] on cerebral CTh measurements. A higher field strength, multi-echo sequence, more coil channels, harmonization of CTh measurements across scanners and sites, use of homogeneous sets of platforms, and constant operating systems would reduce the bias and improve the reproducibility.

In addition, image processing-related factors might have produced inconsistent results as well. For instance, head motions in patients with PD during imaging and image artifacts induce a consistent bias in morphometric measurements [94], thus signifying the need for quality control to achieve reliable results [95, 96]. However, more than half of the studies included in our CBMA did not perform or specify a visual check and/or a secondary manual intervention for quality control. Furthermore, these studies used different processing pipelines and software packages (different versions of FreeSurfer, CIVET, and CAT12) for estimating CTh, which could have introduced bias. Similarly, a previous work reported differences in measurement between FreeSurfer version v5.0.0 and the two earlier versions (v4.3.1 and v4.5.0) [92]. Other studies demonstrated both commonalities and differences in CTh measurements between FreeSurfer and CIVET [97–99] and between FreeSurfer and CAT12 [100, 101].

With every modification and improvement in algorithms, the performance of various software packages should be evaluated [73]. Surface-based smoothing reduces noise, increases comparability across subjects, and compensates for subtle misalignments caused by image distortion [73]. The extent of smoothing applied to CTh maps critically affects the sensitivity, anatomical precision, and resolution of measurements [102]. The fact that studies included in the meta-analysis employed variable smoothing kernels in the CTh analysis could have overinterpreted the results. Thus, an optimal kernel smoothing method using a hierarchical approach based on sequential statistical thresholding was proposed [102]. As mentioned above, age and gender were associated with CTh alterations. During statistical analysis, a regression model should leave out confounding variables. However, some of the included studies did not treat them as covariates in the statistical models. In addition, an uncorrected threshold may produce spurious results in neuroimaging. Correction for multiple comparisons is essential.

A small sample size results in low statistical power, making it difficult to detect subtle differences and undermining the reliability of results [103]. Sample size estimates were heterogeneous over the cortical surface [104]. A detection of a 0.25-mm CTh difference (10% change in CTh) requires approximately 50 subjects per

group [104]. Similarly, a more subtle detection of a 0.125-mm CTh difference (5% change in CTh) requires more than 250 subjects per group [104]. In line with these numbers, 47 out of the 57 datasets included in the CBMA enrolled less than 50 patients, with no dataset including more than 250 patients. The majority of these studies failed to detect CTh differences between patients with PD and HCs. Therefore, a priori power analysis should be performed to determine an appropriate sample size [105]. Furthermore, pooling multi-site large-sample datasets using standardized imaging protocols, and processing and analysis pipelines, like the PPMI, and Alzheimer's Disease Neuroimaging Initiative (ADNI), becomes increasingly important and should be highly recommended to generate reliable results.

The present CBMA had several limitations. We could not conduct additional subgroup CBMA due to the low number of studies in each PD subtype. When adequate qualified and reliable CTh studies are available for subtyping PD in the future, we may obtain more insights into the cortical characteristics relating to PD. The current evidence of lack consistency of CTh alterations in PD comes from the CBMA of cross-sectional results. Although several longitudinal studies showed the time effects of CTh alterations in PD [44, 79, 81, 82], more such studies employing large cohorts are warranted to investigate longitudinal CTh alterations to reflect neurodegenerative dynamics. CBMA is a powerful technique to quantitatively integrate neuroimaging studies; however, its algorithms are still evolving [50, 106]. Although we used SDM-PSI, the latest algorithm, the present CBMA relied only on the peak coordinate-related information reported in individual original studies. This limitation could be overcome by using image-based meta-analyses or mixed image- and coordinate-based meta-analyses [54, 106]. Further, despite being a comprehensive CBMA comprising a large pooled sample of PD, certain studies or datasets were excluded because of incomplete information reported. Data sharing and integrity of neuroimaging reports are encouraged in future studies.

Conclusions and future perspectives

The present CBMA detected no evidence of consistent CTh alterations in patients with PD relative to HCs. This could be attributed to underpowered small sample sizes, sample heterogeneity, and variations in imaging methods. The lack of replicability across CTh studies highlights the need to control for potential confounding factors. Future studies should involve appropriate sample size, well-characterized subtype homogeneous samples, pooling of multi-site large-sample datasets, higher field strength, multi-echo sequence, more coil

channels, harmonization of CTh measurements across scanners and sites, homogeneous sets of platforms, constant operating systems, quality control, well-validated algorithms, optimal smoothing kernel, appropriate covariate regression, correction for multiple comparisons, and longitudinal data to investigate CTh alterations in PD and produce robust and replicable results.

MATERIALS AND METHODS

Protocol and registration

The CBMA was performed following the Preferred Reporting Items of Systematic Review and Meta-Analysis (PRISMA) guidelines [107] and the recent guidelines and recommendations for neuroimaging meta-analysis [50, 51]. The protocol of this CBMA was registered at PROSPERO (<http://www.crd.york.ac.uk/PROSPERO>) (registration number: CRD42020148775) and published [108].

Data sources and study selection

PubMed, Embase, and Web of Science databases were comprehensively searched using the following keywords: ((Parkinson disease) OR Parkinson*) AND ((cortical thickness) OR (cortical thinning) OR (surface-based morphometry)) for both English and non-English papers from the database inception to July 1, 2019 and updated on Feb 2, 2020. For studies published in Chinese, China National Knowledge Infrastructure (CNKI), WanFang, and SinoMed databases were also searched. Reference lists of relevant reviews and articles selected for inclusion were further manually searched.

The criteria for including articles in CBMA were: (i) articles on patients with idiopathic PD diagnosed according to the accepted criteria [109–111]; (ii) articles comparing regional CTh differences between patients with idiopathic PD and HC subjects at the whole-brain cortical level; (iii) articles reporting peak coordinates of significant clusters in standard MNI or Talairach space; and (iv) original articles published in a peer-reviewed journal in English or Chinese.

Publications were excluded if: (i) the sample size was less than seven either in the PD group or the HC group [51]; (ii) studies included PD patients with dementia; (iii) studies reported significant results without listing the three-dimensional coordinates; (iv) studies only employed regions of interest analysis, small volume corrections, or other statistical thresholds that varied depending on the brain regions; (v) studies only conducted global CTh analysis; (vi) studies lacked an

HC group; (vii) studies included patient samples overlapping with that with the largest sample size; (viii) studies were longitudinal without baseline comparisons; (ix) publications were not original articles, such as conference abstracts, research protocols, letters, reviews, and editorials.

Quality assessment

There is no objective tool to perform a quality assessment of CTh studies. Referring to a previous work [52], we used a modified 12-point checklist to assess the quality of each included study in the CBMA (Supplementary Table 1). This checklist integrated the items such as the sample characteristics, imaging-specific methodology employed, and results reported in the studies.

Data extraction

The following data were extracted from the included studies: the first author's family name, publication year, sample size, number of male patients, age, education (years), disease duration, UPDRS-III, HY stage, MMSE, LEDD, MR scanner manufacturer and platform, field strength, head coil, MR sequence, voxel size, imaging-processing software package, smooth kernel, statistical model, covariate, statistical threshold, peak coordinates, the height of the peaks (t-value, z-value, and p-value), and their stereotactic reference space.

L.Q.S and P.W.Z independently performed the literature search, study selection, quality assessment, and data extraction. Any inconsistencies or discrepancies were resolved by a consensus discussion.

Data analysis

Main CBMA

The main CBMA was conducted using the SDM-PSI software package (version 6.21, <https://www.sdmproject.com/>). SDM-PSI uses a new algorithm for CBMA that conducts standard voxelwise tests and, importantly, a standard PSI to assess whether effects are not null, rather than a test of convergence in other CBMA methods [53, 54]. The SDM-PSI uses standard statistical procedures to control the familywise error rate [54]. Standard procedures were followed including the preprocessing steps: conversion of peaks to a common MNI space; calculation of maps of lower and upper bounds of possible effect sizes for each study separately based on the peak information using a specific FreeSurfer GM mask [52], full anisotropy = 1, isotropic FWHM = 20mm, and voxel = 2mm; mean analysis: estimation of the most likely effect size and its

standard error based on MetaNSUE algorithms [112, 113], and conducting multiple imputations and meta-analyses using a standard random-effects model and Rubin's rules; FWE correction for multiple comparisons using common permutation tests; and use of TFCE in statistical thresholding ($p < 0.05$ and voxel extent ≥ 10). These procedures have been described in detail previously [53, 54] and in the SDM-PSI reference manual (<https://www.sdmproject.com/manual/>).

Subgroup CBMA

Subgroup CBMA was conducted when the number of datasets was sufficient ($n \geq 10$). Subgroup CBMA would be performed in clinical subtypes (such as PD patients with or without mild cognitive impairment) and imaging methodology variables (including datasets using 3.0 Tesla MRI scanners, slice thickness lower than 1 mm or voxel size lower than $1 \times 1 \times 1$ mm³, FreeSurfer software packages, FWHM of the smoothing kernel size of 15 mm or less, at least one covariate included in the statistical model, and thresholds corrected for multiple comparisons as well as those datasets with quality control of imaging data and those not specifying it).

Jackknife sensitivity, heterogeneity and publication bias analyses

To study the effect of each dataset on the pooled CBMA results, Jackknife sensitivity analysis was performed by iteratively repeating the same analysis K-1 times (K = the number of datasets included), discarding one dataset each time [114, 115].

For every significant cluster with a peak MNI coordinate reported in the main CBMA, information was extracted to derive standard heterogeneity statistics I^2 based on a standard linear hypothesis, with $I^2 < 50\%$ indicating low heterogeneity. The publication bias of the significant brain cluster was assessed using the Egger test ($p < 0.05$).

Meta-regression analysis

Meta-regression analyses were performed to study the potential effects of age, male gender, disease duration, UPDRS-III, HY stage, MMSE, and LEDD on CBMA results. Statistical significance was determined using the TFCE-based FWE corrected threshold ($p < 0.05$ and voxel extent ≥ 10).

AUTHOR CONTRIBUTIONS

JN and JS did analysis and interpretation of data, and manuscript drafting, JHC and HHK did analysis and collection of data, JS, JYK and JHJ did interpretation of data and manuscript drafting. GJK conceived and designed the experiments, and directed manuscript

drafting, financial support and final approval of manuscript.

CONFLICTS OF INTEREST

The authors declare that they have no conflicts of interest.

FUNDING

This work was supported by the National Natural Science Foundation of China (81601161) and Jiangsu Commission of Health (LGY2018039, QNRC 2016466).

REFERENCES

1. Ascherio A, Schwarzschild MA. The epidemiology of Parkinson's disease: risk factors and prevention. *Lancet Neurol.* 2016; 15:1257–72. [https://doi.org/10.1016/S1474-4422\(16\)30230-7](https://doi.org/10.1016/S1474-4422(16)30230-7) PMID:[27751556](https://pubmed.ncbi.nlm.nih.gov/27751556/)
2. GBD 2015 Neurological Disorders Collaborator Group. Global, regional, and national burden of neurological disorders during 1990-2015: a systematic analysis for the global burden of disease study 2015. *Lancet Neurol.* 2017; 16:877–97. [https://doi.org/10.1016/S1474-4422\(17\)30299-5](https://doi.org/10.1016/S1474-4422(17)30299-5) PMID:[28931491](https://pubmed.ncbi.nlm.nih.gov/28931491/)
3. Dorsey ER, Elbaz A, Nichols E, Abd-Allah F, Abdelalim A, Adsuar JC, Ansha MG, Brayne C, Choi JYJ, Collado-Mateo D, Dahodwala N, Do HP, Edessa D, et al. Global, regional, and national burden of Parkinson's disease, 1990–2016: a systematic analysis for the Global Burden of Disease Study 2016. *Lancet Neurol.* 2018; 17:939–53. [https://doi.org/10.1016/S1474-4422\(18\)30295-3](https://doi.org/10.1016/S1474-4422(18)30295-3)
4. Marras C, Chaudhuri KR. Nonmotor features of Parkinson's disease subtypes. *Mov Disord.* 2016; 31:1095–102. <https://doi.org/10.1002/mds.26510> PMID:[26861861](https://pubmed.ncbi.nlm.nih.gov/26861861/)
5. Sauerbier A, Jenner P, Todorova A, Chaudhuri KR. Non motor subtypes and Parkinson's disease. *Parkinsonism Relat Disord.* 2016 (Suppl 1); 22:S41–46. <https://doi.org/10.1016/j.parkreldis.2015.09.027> PMID:[26459660](https://pubmed.ncbi.nlm.nih.gov/26459660/)
6. Helmich RC, Vaillancourt DE, Brooks DJ. The future of brain imaging in Parkinson's disease. *J Parkinsons Dis.* 2018; 8:S47–51. <https://doi.org/10.3233/JPD-181482> PMID:[30584163](https://pubmed.ncbi.nlm.nih.gov/30584163/)
7. Prodoehl J, Burciu RG, Vaillancourt DE. Resting state functional magnetic resonance imaging in Parkinson's disease. *Curr Neurol Neurosci Rep.* 2014; 14:448. <https://doi.org/10.1007/s11910-014-0448-6> PMID:[24744021](https://pubmed.ncbi.nlm.nih.gov/24744021/)
8. Moustafa AA, Chakravarthy S, Phillips JR, Gupta A, Keri S, Polner B, Frank MJ, Jahanshahi M. Motor symptoms in Parkinson's disease: a unified framework. *Neurosci Biobehav Rev.* 2016; 68:727–40. <https://doi.org/10.1016/j.neubiorev.2016.07.010> PMID:[27422450](https://pubmed.ncbi.nlm.nih.gov/27422450/)
9. Weingarten CP, Sundman MH, Hickey P, Chen NK. Neuroimaging of Parkinson's disease: expanding views. *Neurosci Biobehav Rev.* 2015; 59:16–52. <https://doi.org/10.1016/j.neubiorev.2015.09.007> PMID:[26409344](https://pubmed.ncbi.nlm.nih.gov/26409344/)
10. Salat D, Noyce AJ, Schrag A, Tolosa E. Challenges of modifying disease progression in prediagnostic Parkinson's disease. *Lancet Neurol.* 2016; 15:637–48. [https://doi.org/10.1016/S1474-4422\(16\)00060-0](https://doi.org/10.1016/S1474-4422(16)00060-0) PMID:[26993435](https://pubmed.ncbi.nlm.nih.gov/26993435/)
11. Strafella AP, Bohnen NI, Pavese N, Vaillancourt DE, van Eimeren T, Politis M, Tessitore A, Ghadery C, Lewis S, and IPMDS-Neuroimaging Study Group. Imaging markers of progression in Parkinson's disease. *Mov Disord Clin Pract.* 2018; 5:586–96. <https://doi.org/10.1002/mdc3.12673> PMID:[30637278](https://pubmed.ncbi.nlm.nih.gov/30637278/)
12. Prange S, Metereau E, Thobois S. Structural imaging in Parkinson's disease: new developments. *Curr Neurol Neurosci Rep.* 2019; 19:50. <https://doi.org/10.1007/s11910-019-0964-5> PMID:[31214847](https://pubmed.ncbi.nlm.nih.gov/31214847/)
13. Braak H, Del Tredici K, Rüb U, de Vos RA, Jansen Steur EN, Braak E. Staging of brain pathology related to sporadic Parkinson's disease. *Neurobiol Aging.* 2003; 24:197–211. [https://doi.org/10.1016/s0197-4580\(02\)00065-9](https://doi.org/10.1016/s0197-4580(02)00065-9) PMID:[12498954](https://pubmed.ncbi.nlm.nih.gov/12498954/)
14. Hutton C, Draganski B, Ashburner J, Weiskopf N. A comparison between voxel-based cortical thickness and voxel-based morphometry in normal aging. *Neuroimage.* 2009; 48:371–80. <https://doi.org/10.1016/j.neuroimage.2009.06.043> PMID:[19559801](https://pubmed.ncbi.nlm.nih.gov/19559801/)
15. Pereira JB, Ibarretxe-Bilbao N, Marti MJ, Compta Y, Junqué C, Bargallo N, Tolosa E. Assessment of cortical degeneration in patients with Parkinson's disease by voxel-based morphometry, cortical folding, and cortical thickness. *Hum Brain Mapp.* 2012; 33:2521–34. <https://doi.org/10.1002/hbm.21378> PMID:[21898679](https://pubmed.ncbi.nlm.nih.gov/21898679/)
16. Uribe C, Segura B, Baggio HC, Abos A, Garcia-Diaz AI, Campabadal A, Marti MJ, Valldeoriola F, Compta Y, Bargallo N, Junque C. Gray/white matter contrast in Parkinson's disease. *Front Aging Neurosci.* 2018; 10:89.

<https://doi.org/10.3389/fnagi.2018.00089>

PMID:[29636679](https://pubmed.ncbi.nlm.nih.gov/29636679/)

17. Kunst J, Marecek R, Klobusiakova P, Balazova Z, Anderkova L, Nemcova-Elfmarkova N, Rektorova I. Patterns of grey matter atrophy at different stages of Parkinson's and Alzheimer's diseases and relation to cognition. *Brain Topogr.* 2019; 32:142–60.
<https://doi.org/10.1007/s10548-018-0675-2>
PMID:[30206799](https://pubmed.ncbi.nlm.nih.gov/30206799/)
18. Cerasa A, Salsone M, Morelli M, Pugliese P, Arabia G, Gioia CM, Novellino F, Quattrone A. Age at onset influences neurodegenerative processes underlying PD with levodopa-induced dyskinesias. *Parkinsonism Relat Disord.* 2013; 19:883–88.
<https://doi.org/10.1016/j.parkreldis.2013.05.015>
PMID:[23769805](https://pubmed.ncbi.nlm.nih.gov/23769805/)
19. Claassen DO, Dobolyi DG, Isaacs DA, Roman OC, Herb J, Wylie SA, Neimat JS, Donahue MJ, Hedera P, Zald DH, Landman BA, Bowman AB, Dawant BM, Rane S. Linear and curvilinear trajectories of cortical loss with advancing age and disease duration in Parkinson's disease. *Aging Dis.* 2016; 7:220–29.
<https://doi.org/10.14336/AD.2015.1110>
PMID:[27330836](https://pubmed.ncbi.nlm.nih.gov/27330836/)
20. Wilson H, Niccolini F, Pellicano C, Politis M. Cortical thinning across Parkinson's disease stages and clinical correlates. *J Neurol Sci.* 2019; 398:31–38.
<https://doi.org/10.1016/j.jns.2019.01.020>
PMID:[30682518](https://pubmed.ncbi.nlm.nih.gov/30682518/)
21. Lyoo CH, Ryu YH, Lee MS. Cerebral cortical areas in which thickness correlates with severity of motor deficits of Parkinson's disease. *J Neurol.* 2011; 258:1871–76.
<https://doi.org/10.1007/s00415-011-6045-6>
PMID:[21512741](https://pubmed.ncbi.nlm.nih.gov/21512741/)
22. Jubault T, Gagnon JF, Karama S, Ptito A, Lafontaine AL, Evans AC, Monchi O. Patterns of cortical thickness and surface area in early Parkinson's disease. *Neuroimage.* 2011; 55:462–67.
<https://doi.org/10.1016/j.neuroimage.2010.12.043>
PMID:[21184830](https://pubmed.ncbi.nlm.nih.gov/21184830/)
23. Hanganu A, Bedetti C, Jubault T, Gagnon JF, Mejia-Constain B, Degroot C, Lafontaine AL, Chouinard S, Monchi O. Mild cognitive impairment in patients with Parkinson's disease is associated with increased cortical degeneration. *Mov Disord.* 2013; 28:1360–69.
<https://doi.org/10.1002/mds.25541> PMID:[23801590](https://pubmed.ncbi.nlm.nih.gov/23801590/)
24. Yadav SK, Kathiresan N, Mohan S, Vasileiou G, Singh A, Kaura D, Melhem ER, Gupta RK, Wang E, Marincola FM, Borthakur A, Haris M. Gender-based analysis of cortical thickness and structural connectivity in Parkinson's disease. *J Neurol.* 2016; 263:2308–18.
<https://doi.org/10.1007/s00415-016-2308-1>
PMID:[27544505](https://pubmed.ncbi.nlm.nih.gov/27544505/)
25. Gao Y, Nie K, Mei M, Guo M, Huang Z, Wang L, Zhao J, Huang B, Zhang Y, Wang L. Changes in cortical thickness in patients with early Parkinson's disease at different hoehn and yahr stages. *Front Hum Neurosci.* 2018; 12:469.
<https://doi.org/10.3389/fnhum.2018.00469>
PMID:[30542273](https://pubmed.ncbi.nlm.nih.gov/30542273/)
26. Kim JS, Yang JJ, Lee JM, Youn J, Kim JM, Cho JW. Topographic pattern of cortical thinning with consideration of motor laterality in Parkinson disease. *Parkinsonism Relat Disord.* 2014; 20:1186–90.
<https://doi.org/10.1016/j.parkreldis.2014.08.021>
PMID:[25231669](https://pubmed.ncbi.nlm.nih.gov/25231669/)
27. Zarei M, Ibarretxe-Bilbao N, Compta Y, Hough M, Junque C, Bargallo N, Tolosa E, Martí MJ. Cortical thinning is associated with disease stages and dementia in Parkinson's disease. *J Neurol Neurosurg Psychiatry.* 2013; 84:875–81.
<https://doi.org/10.1136/jnnp-2012-304126>
PMID:[23463873](https://pubmed.ncbi.nlm.nih.gov/23463873/)
28. Biundo R, Calabrese M, Weis L, Facchini S, Ricchieri G, Gallo P, Antonini A. Anatomical correlates of cognitive functions in early Parkinson's disease patients. *PLoS One.* 2013; 8:e64222.
<https://doi.org/10.1371/journal.pone.0064222>
PMID:[23717572](https://pubmed.ncbi.nlm.nih.gov/23717572/)
29. Pellicano C, Assogna F, Piras F, Caltagirone C, Pontieri FE, Spalletta G. Regional cortical thickness and cognitive functions in non-demented Parkinson's disease patients: a pilot study. *Eur J Neurol.* 2012; 19:172–75.
<https://doi.org/10.1111/j.1468-1331.2011.03465.x>
PMID:[21771199](https://pubmed.ncbi.nlm.nih.gov/21771199/)
30. Segura B, Baggio HC, Marti MJ, Valldeoriola F, Compta Y, Garcia-Diaz AI, Vendrell P, Bargallo N, Tolosa E, Junque C. Cortical thinning associated with mild cognitive impairment in Parkinson's disease. *Mov Disord.* 2014; 29:1495–503.
<https://doi.org/10.1002/mds.25982> PMID:[25100674](https://pubmed.ncbi.nlm.nih.gov/25100674/)
31. Pagonabarraga J, Corcuera-Solano I, Vives-Gilabert Y, Llebaria G, García-Sánchez C, Pascual-Sedano B, Delfino M, Kulisevsky J, Gómez-Ansón B. Pattern of regional cortical thinning associated with cognitive deterioration in Parkinson's disease. *PLoS One.* 2013; 8:e54980.
<https://doi.org/10.1371/journal.pone.0054980>
PMID:[23359616](https://pubmed.ncbi.nlm.nih.gov/23359616/)
32. Pereira JB, Svenningsson P, Weintraub D, Brønneck K, Lebedev A, Westman E, Aarsland D. Initial cognitive decline is associated with cortical thinning in early Parkinson disease. *Neurology.* 2014; 82:2017–25.
<https://doi.org/10.1213/WNL.0b013e3182911111>
PMID:[24711111](https://pubmed.ncbi.nlm.nih.gov/24711111/)

<https://doi.org/10.1212/WNL.0000000000000483>

PMID:[24808018](https://pubmed.ncbi.nlm.nih.gov/24808018/)

33. Zhang L, Wang M, Sterling NW, Lee EY, Eslinger PJ, Wagner D, Du G, Lewis MM, Truong Y, Bowman FD, Huang X. Cortical thinning and cognitive impairment in Parkinson's disease without dementia. *IEEE/ACM Trans Comput Biol Bioinform.* 2018; 15:570–80.
<https://doi.org/10.1109/TCBB.2015.2465951>
PMID:[29610105](https://pubmed.ncbi.nlm.nih.gov/29610105/)
34. Gasca-Salas C, García-Lorenzo D, Garcia-Garcia D, Clavero P, Obeso JA, Lehericy S, Rodríguez-Oroz MC. Parkinson's disease with mild cognitive impairment: severe cortical thinning antedates dementia. *Brain Imaging Behav.* 2019; 13:180–88.
<https://doi.org/10.1007/s11682-017-9751-6>
PMID:[28710667](https://pubmed.ncbi.nlm.nih.gov/28710667/)
35. Biundo R, Weis L, Facchini S, Formento-Dojot P, Vallengunga A, Pilleri M, Weintraub D, Antonini A. Patterns of cortical thickness associated with impulse control disorders in Parkinson's disease. *Mov Disord.* 2015; 30:688–95.
<https://doi.org/10.1002/mds.26154> PMID:[25649923](https://pubmed.ncbi.nlm.nih.gov/25649923/)
36. Tessitore A, Santangelo G, De Micco R, Vitale C, Giordano A, Raimo S, Corbo D, Amboni M, Barone P, Tedeschi G. Cortical thickness changes in patients with Parkinson's disease and impulse control disorders. *Parkinsonism Relat Disord.* 2016; 24:119–25.
<https://doi.org/10.1016/j.parkreldis.2015.10.013>
PMID:[26810913](https://pubmed.ncbi.nlm.nih.gov/26810913/)
37. Huang P, Lou Y, Xuan M, Gu Q, Guan X, Xu X, Song Z, Luo W, Zhang M. Cortical abnormalities in Parkinson's disease patients and relationship to depression: a surface-based morphometry study. *Psychiatry Res Neuroimaging.* 2016; 250:24–28.
<https://doi.org/10.1016/j.psychres.2016.03.002>
PMID:[27107157](https://pubmed.ncbi.nlm.nih.gov/27107157/)
38. Luo C, Song W, Chen Q, Yang J, Gong Q, Shang HF. Cortical thinning in drug-naïve Parkinson's disease patients with depression. *J Neurol.* 2016; 263:2114–19.
<https://doi.org/10.1007/s00415-016-8241-x>
PMID:[27485171](https://pubmed.ncbi.nlm.nih.gov/27485171/)
39. Zanigni S, Sambati L, Evangelisti S, Testa C, Calandra-Buonaura G, Manners DN, Terlizzi R, Poda R, Oppi F, Lodi R, Cortelli P, Tonon C, and BoProPark Study Group. Precuneal thickness and depression in Parkinson disease. *Neurodegener Dis.* 2017; 17:97–102.
<https://doi.org/10.1159/000450614> PMID:[27883992](https://pubmed.ncbi.nlm.nih.gov/27883992/)
40. Campabadal A, Uribe C, Segura B, Baggio HC, Abos A, Garcia-Diaz AI, Marti MJ, Valldeoriola F, Compta Y, Bargallo N, Junque C. Brain correlates of progressive olfactory loss in Parkinson's disease. *Parkinsonism Relat Disord.* 2017; 41:44–50.
<https://doi.org/10.1016/j.parkreldis.2017.05.005>
PMID:[28522171](https://pubmed.ncbi.nlm.nih.gov/28522171/)
41. Rahayel S, Gaubert M, Postuma RB, Montplaisir J, Carrier J, Monchi O, Rémillard-Pelchat D, Bourgouin PA, Panisset M, Chouinard S, Joubert S, Gagnon JF. Brain atrophy in Parkinson's disease with polysomnography-confirmed REM sleep behavior disorder. *Sleep.* 2019; 42:zsz062.
<https://doi.org/10.1093/sleep/zsz062> PMID:[30854555](https://pubmed.ncbi.nlm.nih.gov/30854555/)
42. Polli A, Weis L, Biundo R, Thacker M, Turolla A, Koutsikos K, Chaudhuri KR, Antonini A. Anatomical and functional correlates of persistent pain in Parkinson's disease. *Mov Disord.* 2016; 31:1854–64.
<https://doi.org/10.1002/mds.26826> PMID:[27704616](https://pubmed.ncbi.nlm.nih.gov/27704616/)
43. Yoon EJ, Ismail Z, Hanganu A, Kibreab M, Hammer T, Cheetham J, Kathol I, Sarna JR, Martino D, Furtado S, Monchi O. Mild behavioral impairment is linked to worse cognition and brain atrophy in Parkinson disease. *Neurology.* 2019; 93:e766–77.
<https://doi.org/10.1212/WNL.0000000000007968>
PMID:[31320470](https://pubmed.ncbi.nlm.nih.gov/31320470/)
44. Ibarretxe-Bilbao N, Junque C, Segura B, Baggio HC, Marti MJ, Valldeoriola F, Bargallo N, Tolosa E. Progression of cortical thinning in early Parkinson's disease. *Mov Disord.* 2012; 27:1746–53.
<https://doi.org/10.1002/mds.25240> PMID:[23124622](https://pubmed.ncbi.nlm.nih.gov/23124622/)
45. Worker A, Blain C, Jarosz J, Chaudhuri KR, Barker GJ, Williams SC, Brown R, Leigh PN, Simmons A. Cortical thickness, surface area and volume measures in Parkinson's disease, multiple system atrophy and progressive supranuclear palsy. *PLoS One.* 2014; 9:e114167.
<https://doi.org/10.1371/journal.pone.0114167>
PMID:[25463618](https://pubmed.ncbi.nlm.nih.gov/25463618/)
46. Acosta-Cabronero J, Cardenas-Blanco A, Betts MJ, Butryn M, Valdes-Herrera JP, Galazky I, Nestor PJ. The whole-brain pattern of magnetic susceptibility perturbations in Parkinson's disease. *Brain.* 2017; 140:118–31.
<https://doi.org/10.1093/brain/aww278>
PMID:[27836833](https://pubmed.ncbi.nlm.nih.gov/27836833/)
47. Mak E, Su L, Williams GB, Firbank MJ, Lawson RA, Yarnall AJ, Duncan GW, Owen AM, Khoo TK, Brooks DJ, Rowe JB, Barker RA, Burn DJ, O'Brien JT. Baseline and longitudinal grey matter changes in newly diagnosed Parkinson's disease: ICICLE-PD study. *Brain.* 2015; 138:2974–86.
<https://doi.org/10.1093/brain/awv211>
PMID:[26173861](https://pubmed.ncbi.nlm.nih.gov/26173861/)
48. Yao N, Shek-Kwan Chang R, Cheung C, Pang S, Lau KK, Suckling J, Rowe JB, Yu K, Ka-Fung Mak H, Chua SE, Ho SL, McAlonan GM. The default mode network is

- disrupted in Parkinson's disease with visual hallucinations. *Hum Brain Mapp.* 2014; 35:5658–66. <https://doi.org/10.1002/hbm.22577> PMID:24985056
49. Kamagata K, Zalesky A, Hatano T, Ueda R, Di Biase MA, Okuzumi A, Shimoji K, Hori M, Caeyenberghs K, Pantelis C, Hattori N, Aoki S. Gray matter abnormalities in idiopathic Parkinson's disease: evaluation by diffusional kurtosis imaging and neurite orientation dispersion and density imaging. *Hum Brain Mapp.* 2017; 38:3704–22. <https://doi.org/10.1002/hbm.23628> PMID:28470878
 50. Müller VI, Cieslik EC, Laird AR, Fox PT, Radua J, Mataix-Cols D, Tench CR, Yarkoni T, Nichols TE, Turkeltaub PE, Wager TD, Eickhoff SB. Ten simple rules for neuroimaging meta-analysis. *Neurosci Biobehav Rev.* 2018; 84:151–61. <https://doi.org/10.1016/j.neubiorev.2017.11.012> PMID:29180258
 51. Tahmasian M, Sepehry AA, Samea F, Khodadadifar T, Soltaninejad Z, Javaheripour N, Khazaie H, Zarei M, Eickhoff SB, Eickhoff CR. Practical recommendations to conduct a neuroimaging meta-analysis for neuropsychiatric disorders. *Hum Brain Mapp.* 2019; 40:5142–54. <https://doi.org/10.1002/hbm.24746> PMID:31379049
 52. Li Q, Zhao Y, Chen Z, Long J, Dai J, Huang X, Lui S, Radua J, Vieta E, Kemp GJ, Sweeney JA, Li F, Gong Q. Meta-analysis of cortical thickness abnormalities in medication-free patients with major depressive disorder. *Neuropsychopharmacology.* 2020; 45:703–12. <https://doi.org/10.1038/s41386-019-0563-9> PMID:31694045
 53. Albajes-Eizagirre A, Solanes A, Fullana MA, Ioannidis JP, Fusar-Poli P, Torrent C, Solé B, Bonnín CM, Vieta E, Mataix-Cols D, Radua J. Meta-analysis of voxel-based neuroimaging studies using seed-based d mapping with permutation of subject images (SDM-PSI). *J Vis Exp.* 2019. <https://doi.org/10.3791/59841> PMID:31840658
 54. Albajes-Eizagirre A, Solanes A, Vieta E, Radua J. Voxel-based meta-analysis via permutation of subject images (PSI): theory and implementation for SDM. *Neuroimage.* 2019; 186:174–84. <https://doi.org/10.1016/j.neuroimage.2018.10.077> PMID:30389629
 55. Carriere N, Besson P, Dujardin K, Duhamel A, Defebvre L, Delmaire C, Devos D. Apathy in Parkinson's disease is associated with nucleus accumbens atrophy: a magnetic resonance imaging shape analysis. *Mov Disord.* 2014; 29:897–903. <https://doi.org/10.1002/mds.25904> PMID:24817690
 56. Carriere N, Lopes R, Defebvre L, Delmaire C, Dujardin K. Impaired corticostriatal connectivity in impulse control disorders in Parkinson disease. *Neurology.* 2015; 84:2116–23. <https://doi.org/10.1212/WNL.0000000000001619> PMID:25925985
 57. Cerasa A, Morelli M, Augimeri A, Salsone M, Novellino F, Gioia MC, Arabia G, Quattrone A. Prefrontal thickening in PD with levodopa-induced dyskinesias: new evidence from cortical thickness measurement. *Parkinsonism Relat Disord.* 2013; 19:123–25. <https://doi.org/10.1016/j.parkreldis.2012.06.003> PMID:22742954
 58. Chung SJ, Park YH, Yun HJ, Kwon H, Yoo HS, Sohn YH, Lee JM, Lee PH. Clinical relevance of amnesic versus non-amnesic mild cognitive impairment subtyping in Parkinson's disease. *Eur J Neurol.* 2019; 26:766–73. <https://doi.org/10.1111/ene.13886> PMID:30565368
 59. Danti S, Toschi N, Diciotti S, Tessa C, Poletti M, Del Dotto P, Lucetti C. Cortical thickness in de novo patients with Parkinson disease and mild cognitive impairment with consideration of clinical phenotype and motor laterality. *Eur J Neurol.* 2015; 22:1564–72. <https://doi.org/10.1111/ene.12785> PMID:26212370
 60. Deng X, Zhou M, Tang C, Zhang J, Zhu L, Xie Z, Gong H, Xiao X, Xu R. The alterations of cortical volume, thickness, surface, and density in the intermediate sporadic Parkinson's disease from the han population of mainland China. *Front Aging Neurosci.* 2016; 8:185. <https://doi.org/10.3389/fnagi.2016.00185> PMID:27536237
 61. Garcia-Diaz AI, Segura B, Baggio HC, Marti MJ, Valdeoriola F, Compta Y, Bargallo N, Uribe C, Campabadal A, Abos A, Junque C. Structural brain correlations of visuospatial and visuoperceptual tests in Parkinson's disease. *J Int Neuropsychol Soc.* 2018; 24:33–44. <https://doi.org/10.1017/S1355617717000583> PMID:28714429
 62. Garcia-Diaz AI, Segura B, Baggio HC, Marti MJ, Valdeoriola F, Compta Y, Vendrell P, Bargallo N, Tolosa E, Junque C. Structural MRI correlates of the MMSE and pentagon copying test in Parkinson's disease. *Parkinsonism Relat Disord.* 2014; 20:1405–10. <https://doi.org/10.1016/j.parkreldis.2014.10.014> PMID:25457818
 63. Gerrits NJ, van Loenhoud AC, van den Berg SF, Berendse HW, Foncke EM, Klein M, Stoffers D, van der Werf YD, van den Heuvel OA. Cortical thickness, surface area and subcortical volume differentially contribute to cognitive heterogeneity in Parkinson's disease. *PLoS One.* 2016; 11:e0148852.

- <https://doi.org/10.1371/journal.pone.0148852>
PMID:[26919667](https://pubmed.ncbi.nlm.nih.gov/26919667/)
64. Guimarães RP, Arci Santos MC, Dagher A, Campos LS, Azevedo P, Piovesana LG, De Campos BM, Larcher K, Zeighami Y, Scarparo Amato-Filho AC, Cendes F, D'Abreu AC. Pattern of reduced functional connectivity and structural abnormalities in Parkinson's disease: an exploratory study. *Front Neurol*. 2017; 7:243.
<https://doi.org/10.3389/fneur.2016.00243>
PMID:[28133455](https://pubmed.ncbi.nlm.nih.gov/28133455/)
65. Lyoo CH, Ryu YH, Lee MS. Topographical distribution of cerebral cortical thinning in patients with mild Parkinson's disease without dementia. *Mov Disord*. 2010; 25:496–99.
<https://doi.org/10.1002/mds.22975> PMID:[20108369](https://pubmed.ncbi.nlm.nih.gov/20108369/)
66. Madhyastha TM, Askren MK, Boord P, Zhang J, Leverenz JB, Grabowski TJ. Cerebral perfusion and cortical thickness indicate cortical involvement in mild Parkinson's disease. *Mov Disord*. 2015; 30:1893–900.
<https://doi.org/10.1002/mds.26128> PMID:[25759166](https://pubmed.ncbi.nlm.nih.gov/25759166/)
67. Nürnberger L, Gracien RM, Hok P, Hof SM, Rüb U, Steinmetz H, Hilker R, Klein JC, Deichmann R, Baudrexel S. Longitudinal changes of cortical microstructure in Parkinson's disease assessed with T1 relaxometry. *Neuroimage Clin*. 2016; 13:405–14.
<https://doi.org/10.1016/j.nicl.2016.12.025>
PMID:[28116233](https://pubmed.ncbi.nlm.nih.gov/28116233/)
68. Pereira JB, Weintraub D, Chahine L, Aarsland D, Hansson O, Westman E. Cortical thinning in patients with REM sleep behavior disorder is associated with clinical progression. *NPJ Parkinsons Dis*. 2019; 5:7.
<https://doi.org/10.1038/s41531-019-0079-3>
PMID:[31069252](https://pubmed.ncbi.nlm.nih.gov/31069252/)
69. Xiang Y, Shen Q, Tan C. The Cortical Thickness in Early-onset and Late-onset Parkinson's Disease. *Clin Radiol*. 2019; 38:1584–88.
70. Yoo HS, Yun HJ, Chung SJ, Sunwoo MK, Lee JM, Sohn YH, Lee PH. Patterns of neuropsychological profile and cortical thinning in Parkinson's disease with punding. *PLoS One*. 2015; 10:e0134468.
<https://doi.org/10.1371/journal.pone.0134468>
PMID:[26218765](https://pubmed.ncbi.nlm.nih.gov/26218765/)
71. Gorgolewski KJ, Poldrack RA. A practical guide for improving transparency and reproducibility in neuroimaging research. *PLoS Biol*. 2016; 14:e1002506.
<https://doi.org/10.1371/journal.pbio.1002506>
PMID:[27389358](https://pubmed.ncbi.nlm.nih.gov/27389358/)
72. Cardinale F, Chinnici G, Bramerio M, Mai R, Sartori I, Cossu M, Lo Russo G, Castana L, Colombo N, Caborni C, De Momi E, Ferrigno G. Validation of FreeSurfer-estimated brain cortical thickness: comparison with histologic measurements. *Neuroinformatics*. 2014; 12:535–42.
<https://doi.org/10.1007/s12021-014-9229-2>
PMID:[24789776](https://pubmed.ncbi.nlm.nih.gov/24789776/)
73. Wagstyl K, Lerch JP. Cortical thickness. *Brain morphometry*: Springer. 2018; 106:35–49.
https://doi.org/10.1007/978-1-4939-7647-8_3
74. Erro R, Vitale C, Amboni M, Picillo M, Moccia M, Longo K, Santangelo G, De Rosa A, Allocca R, Giordano F, Orefice G, De Michele G, Santoro L, et al. The heterogeneity of early Parkinson's disease: a cluster analysis on newly diagnosed untreated patients. *PLoS One*. 2013; 8:e70244.
<https://doi.org/10.1371/journal.pone.0070244>
PMID:[23936396](https://pubmed.ncbi.nlm.nih.gov/23936396/)
75. Kang JH, Mollenhauer B, Coffey CS, Toledo JB, Weintraub D, Galasko DR, Irwin DJ, Van Deerlin V, Chen-Plotkin AS, Caspell-Garcia C, Waligórska T, Taylor P, Shah N, et al, and Parkinson's Progression Marker Initiative. CSF biomarkers associated with disease heterogeneity in early Parkinson's disease: the Parkinson's progression markers initiative study. *Acta Neuropathol*. 2016; 131:935–49.
<https://doi.org/10.1007/s00401-016-1552-2>
PMID:[27021906](https://pubmed.ncbi.nlm.nih.gov/27021906/)
76. Selikhova M, Williams DR, Kempster PA, Holton JL, Revesz T, Lees AJ. A clinico-pathological study of subtypes in Parkinson's disease. *Brain*. 2009; 132:2947–57.
<https://doi.org/10.1093/brain/awp234>
PMID:[19759203](https://pubmed.ncbi.nlm.nih.gov/19759203/)
77. von Coelln R, Shulman LM. Clinical subtypes and genetic heterogeneity: of lumping and splitting in Parkinson disease. *Curr Opin Neurol*. 2016; 29:727–34.
<https://doi.org/10.1097/WCO.0000000000000384>
PMID:[27749396](https://pubmed.ncbi.nlm.nih.gov/27749396/)
78. Chung SJ, Park YH, Yoo HS, Lee YH, Ye BS, Sohn YH, Lee JM, Lee PH. Mild cognitive impairment reverts have a favorable cognitive prognosis and cortical integrity in Parkinson's disease. *Neurobiol Aging*. 2019; 78:168–77.
<https://doi.org/10.1016/j.neurobiolaging.2019.02.023>
PMID:[30947112](https://pubmed.ncbi.nlm.nih.gov/30947112/)
79. Sampedro F, Marín-Lahoz J, Martínez-Horta S, Pagonabarraga J, Kulisevsky J. Pattern of cortical thinning associated with the BDNF Val66Met polymorphism in Parkinson's disease. *Behav Brain Res*. 2019; 372:112039.
<https://doi.org/10.1016/j.bbr.2019.112039>
PMID:[31202861](https://pubmed.ncbi.nlm.nih.gov/31202861/)
80. Uribe C, Segura B, Baggio HC, Abos A, Marti MJ, Valdeoriola F, Compta Y, Bargallo N, Junque C.

- Patterns of cortical thinning in nondemented Parkinson's disease patients. *Mov Disord.* 2016; 31:699–708.
<https://doi.org/10.1002/mds.26590> PMID:[27094093](https://pubmed.ncbi.nlm.nih.gov/27094093/)
81. Uribe C, Segura B, Baggio HC, Abos A, Garcia-Diaz AI, Campabadal A, Marti MJ, Valldeoriola F, Compta Y, Bargallo N, Junque C. Progression of Parkinson's disease patients' subtypes based on cortical thinning: 4-year follow-up. *Parkinsonism Relat Disord.* 2019; 64:286–92.
<https://doi.org/10.1016/j.parkreldis.2019.05.012> PMID:[31103485](https://pubmed.ncbi.nlm.nih.gov/31103485/)
82. Sampedro F, Martínez-Horta S, Marín-Lahoz J, Pagonabarraga J, Kulisevsky J. Longitudinal intracortical diffusivity changes in de-novo Parkinson's disease: a promising imaging biomarker. *Parkinsonism Relat Disord.* 2019; 68:22–25.
<https://doi.org/10.1016/j.parkreldis.2019.09.031> PMID:[31621613](https://pubmed.ncbi.nlm.nih.gov/31621613/)
83. Fortin JP, Cullen N, Sheline YI, Taylor WD, Aselcioglu I, Cook PA, Adams P, Cooper C, Fava M, McGrath PJ, McInnis M, Phillips ML, Trivedi MH, et al. Harmonization of cortical thickness measurements across scanners and sites. *Neuroimage.* 2018; 167:104–20.
<https://doi.org/10.1016/j.neuroimage.2017.11.024> PMID:[29155184](https://pubmed.ncbi.nlm.nih.gov/29155184/)
84. Yang CY, Liu HM, Chen SK, Chen YF, Lee CW, Yeh LR. Reproducibility of brain morphometry from short-term repeat clinical MRI examinations: a retrospective study. *PLoS One.* 2016; 11:e0146913.
<https://doi.org/10.1371/journal.pone.0146913> PMID:[26812647](https://pubmed.ncbi.nlm.nih.gov/26812647/)
85. Han X, Jovicich J, Salat D, van der Kouwe A, Quinn B, Czanner S, Busa E, Pacheco J, Albert M, Killiany R, Maguire P, Rosas D, Makris N, et al. Reliability of MRI-derived measurements of human cerebral cortical thickness: the effects of field strength, scanner upgrade and manufacturer. *Neuroimage.* 2006; 32:180–94.
<https://doi.org/10.1016/j.neuroimage.2006.02.051> PMID:[16651008](https://pubmed.ncbi.nlm.nih.gov/16651008/)
86. Lüsebrink F, Wollrab A, Speck O. Cortical thickness determination of the human brain using high resolution 3T and 7T MRI data. *Neuroimage.* 2013; 70:122–31.
<https://doi.org/10.1016/j.neuroimage.2012.12.016> PMID:[23261638](https://pubmed.ncbi.nlm.nih.gov/23261638/)
87. Park HJ, Youn T, Jeong SO, Oh MK, Kim SY, Kim EY. SENSE factors for reliable cortical thickness measurement. *Neuroimage.* 2008; 40:187–96.
<https://doi.org/10.1016/j.neuroimage.2007.11.013> PMID:[18096408](https://pubmed.ncbi.nlm.nih.gov/18096408/)
88. Yan S, Qian T, Maréchal B, Kober T, Zhang X, Zhu J, Lei J, Li M, Jin Z. Test-retest variability of brain morphometry analysis: an investigation of sequence and coil effects. *Ann Transl Med.* 2020; 8:12.
<https://doi.org/10.21037/atm.2019.11.149> PMID:[32055603](https://pubmed.ncbi.nlm.nih.gov/32055603/)
89. Wonderlick JS, Ziegler DA, Hosseini-Varnamkhasti P, Locascio JJ, Bakkour A, van der Kouwe A, Triantafyllou C, Corkin S, Dickerson BC. Reliability of MRI-derived cortical and subcortical morphometric measures: effects of pulse sequence, voxel geometry, and parallel imaging. *Neuroimage.* 2009; 44:1324–33.
<https://doi.org/10.1016/j.neuroimage.2008.10.037> PMID:[19038349](https://pubmed.ncbi.nlm.nih.gov/19038349/)
90. Melzer TR, Keenan RJ, Leeper GJ, Kingston-Smith S, Felton SA, Green SK, Henderson KJ, Palmer NJ, Shoorangiz R, Almuqbel MM, Myall DJ. Test-retest reliability and sample size estimates after MRI scanner relocation. *Neuroimage.* 2020; 211:116608.
<https://doi.org/10.1016/j.neuroimage.2020.116608> PMID:[32032737](https://pubmed.ncbi.nlm.nih.gov/32032737/)
91. Iscan Z, Jin TB, Kendrick A, Szeglin B, Lu H, Trivedi M, Fava M, McGrath PJ, Weissman M, Kurian BT, Adams P, Weyandt S, Touns M, et al. Test-retest reliability of freesurfer measurements within and between sites: effects of visual approval process. *Hum Brain Mapp.* 2015; 36:3472–85.
<https://doi.org/10.1002/hbm.22856> PMID:[26033168](https://pubmed.ncbi.nlm.nih.gov/26033168/)
92. Gronenschild EH, Habets P, Jacobs HI, Mengelers R, Rozendaal N, van Os J, Marcelis M. The effects of FreeSurfer version, workstation type, and macintosh operating system version on anatomical volume and cortical thickness measurements. *PLoS One.* 2012; 7:e38234.
<https://doi.org/10.1371/journal.pone.0038234> PMID:[22675527](https://pubmed.ncbi.nlm.nih.gov/22675527/)
93. Glatard T, Lewis LB, Ferreira da Silva R, Adalat R, Beck N, Lepage C, Rioux P, Rousseau ME, Sherif T, Deelman E, Khalili-Mahani N, Evans AC. Reproducibility of neuroimaging analyses across operating systems. *Front Neuroinform.* 2015; 9:12.
<https://doi.org/10.3389/fninf.2015.00012> PMID:[25964757](https://pubmed.ncbi.nlm.nih.gov/25964757/)
94. Rosen AF, Roalf DR, Ruparel K, Blake J, Seelaus K, Villa LP, Ciric R, Cook PA, Davatzikos C, Elliott MA, Garcia de La Garza A, Gennatas ED, Quarmley M, et al. Quantitative assessment of structural image quality. *Neuroimage.* 2018; 169:407–18.
<https://doi.org/10.1016/j.neuroimage.2017.12.059> PMID:[29278774](https://pubmed.ncbi.nlm.nih.gov/29278774/)
95. Reuter M, Tisdall MD, Qureshi A, Buckner RL, van der Kouwe AJ, Fischl B. Head motion during MRI

- acquisition reduces gray matter volume and thickness estimates. *Neuroimage*. 2015; 107:107–15.
<https://doi.org/10.1016/j.neuroimage.2014.12.006>
PMID:25498430
96. Ducharme S, Albaugh MD, Nguyen TV, Hudziak JJ, Mateos-Pérez JM, Labbe A, Evans AC, Karama S, and Brain Development Cooperative Group. Trajectories of cortical thickness maturation in normal brain development--The importance of quality control procedures. *Neuroimage*. 2016; 125:267–79.
<https://doi.org/10.1016/j.neuroimage.2015.10.010>
PMID:26463175
97. Redolfi A, Manset D, Barkhof F, Wahlund LO, Glatard T, Mangin JF, Frisoni GB, and neuGRID Consortium, for the Alzheimer's Disease Neuroimaging Initiative. Head-to-head comparison of two popular cortical thickness extraction algorithms: a cross-sectional and longitudinal study. *PLoS One*. 2015; 10:e0117692.
<https://doi.org/10.1371/journal.pone.0117692>
PMID:25781983
98. Jeon S, Lepage C, Lewis L, Khalili-Mahani N, Bermudez P, Vincent R, Zijdenbos A, Omidyeganeh M, Adalat R, Evans A. (2017). Reproducibility of Cortical Thickness Measurement: CIVET (v2. 1) vs. FreeSurfer (v6. 0-beta & v5. 3). On Human Brain Mapping Symposium.
99. Lewis L, Lepage C, Khalili-Mahani N, Omidyeganeh M, Jeon S, Bermudez P, Zijdenbos A, Vincent R, Adalat R, Evans A. (2017). Robustness and reliability of cortical surface reconstruction in CIVET and FreeSurfer. On Human Brain Mapping Symposium.
100. Seiger R, Ganger S, Kranz GS, Hahn A, Lanzenberger R. Cortical thickness estimations of FreeSurfer and the CAT12 toolbox in patients with Alzheimer's disease and healthy controls. *J Neuroimaging*. 2018; 28:515–23.
<https://doi.org/10.1111/jon.12521>
PMID:29766613
101. Righart R, Schmidt P, Dahnke R, Biberacher V, Beer A, Buck D, Hemmer B, Kirschke JS, Zimmer C, Gaser C, Mühlau M. Volume versus surface-based cortical thickness measurements: a comparative study with healthy controls and multiple sclerosis patients. *PLoS One*. 2017; 12:e0179590.
<https://doi.org/10.1371/journal.pone.0179590>
PMID:28683072
102. Bernal-Rusiel JL, Atienza M, Cantero JL. Determining the optimal level of smoothing in cortical thickness analysis: a hierarchical approach based on sequential statistical thresholding. *Neuroimage*. 2010; 52:158–71.
<https://doi.org/10.1016/j.neuroimage.2010.03.074>
PMID:20362677
103. Button KS, Ioannidis JP, Mokrysz C, Nosek BA, Flint J, Robinson ES, Munafò MR. Power failure: why small sample size undermines the reliability of neuroscience. *Nat Rev Neurosci*. 2013; 14:365–76.
<https://doi.org/10.1038/nrn3475>
PMID:23571845
104. Pardoe HR, Abbott DF, Jackson GD, and Alzheimer's Disease Neuroimaging Initiative. Sample size estimates for well-powered cross-sectional cortical thickness studies. *Hum Brain Mapp*. 2013; 34:3000–09.
<https://doi.org/10.1002/hbm.22120> PMID:22807270
105. Liem F, Mérillat S, Bezzola L, Hirsiger S, Philipp M, Madhyastha T, Jäncke L. Reliability and statistical power analysis of cortical and subcortical FreeSurfer metrics in a large sample of healthy elderly. *Neuroimage*. 2015; 108:95–109.
<https://doi.org/10.1016/j.neuroimage.2014.12.035>
PMID:25534113
106. Radua J, Mataix-Cols D. Meta-analytic methods for neuroimaging data explained. *Biol Mood Anxiety Disord*. 2012; 2:6.
<https://doi.org/10.1186/2045-5380-2-6>
PMID:22737993
107. Moher D, Liberati A, Tetzlaff J, Altman DG, and PRISMA Group. Preferred reporting items for systematic reviews and meta-analyses: the PRISMA statement. *BMJ*. 2009; 339:b2535
<https://doi.org/10.1136/bmj.b2535> PMID:19622551
108. Sheng L, Zhao P, Ma H, Radua J, Yi Z, Shi Y, Zhong J, Dai Z, Pan P. Cortical thickness in Parkinson disease: a coordinate-based meta-analysis. *Medicine (Baltimore)*. 2020; 99:e21403.
<https://doi.org/10.1097/MD.00000000000021403>
PMID:32756136
109. Postuma RB, Berg D, Stern M, Poewe W, Olanow CW, Oertel W, Obeso J, Marek K, Litvan I, Lang AE, Halliday G, Goetz CG, Gasser T, et al. MDS clinical diagnostic criteria for Parkinson's disease. *Mov Disord*. 2015; 30:1591–601.
<https://doi.org/10.1002/mds.26424>
PMID:26474316
110. Gelb DJ, Oliver E, Gilman S. Diagnostic criteria for Parkinson disease. *Arch Neurol*. 1999; 56:33–39.
<https://doi.org/10.1001/archneur.56.1.33>
PMID:9923759
111. Gibb WR, Lees AJ. The relevance of the lewy body to the pathogenesis of idiopathic Parkinson's disease. *J Neurol Neurosurg Psychiatry*. 1988; 51:745–52.
<https://doi.org/10.1136/jnnp.51.6.745> PMID:2841426
112. Radua J, Schmidt A, Borgwardt S, Heinz A, Schlagenhauf F, McGuire P, Fusar-Poli P. Ventral striatal activation during reward processing in

psychosis: a neurofunctional meta-analysis. *JAMA Psychiatry*. 2015; 72:1243–51.

<https://doi.org/10.1001/jamapsychiatry.2015.2196>

PMID:[26558708](https://pubmed.ncbi.nlm.nih.gov/26558708/)

113. Albajes-Eizagirre A, Solanes A, Radua J. Meta-analysis of non-statistically significant unreported effects. *Stat Methods Med Res*. 2019; 28:3741–54.

<https://doi.org/10.1177/0962280218811349>

PMID:[30514161](https://pubmed.ncbi.nlm.nih.gov/30514161/)

114. Radua J, Mataix-Cols D. Voxel-wise meta-analysis of grey matter changes in obsessive-compulsive disorder. *Br J Psychiatry*. 2009; 195:393–402.

<https://doi.org/10.1192/bjp.bp.108.055046>

PMID:[19880927](https://pubmed.ncbi.nlm.nih.gov/19880927/)

115. Radua J, Rubia K, Canales-Rodríguez EJ, Pomarol-Clotet E, Fusar-Poli P, Mataix-Cols D. Anisotropic kernels for coordinate-based meta-analyses of neuroimaging studies. *Front Psychiatry*. 2014; 5:13.

<https://doi.org/10.3389/fpsy.2014.00013>

PMID:[24575054](https://pubmed.ncbi.nlm.nih.gov/24575054/)

SUPPLEMENTARY MATERIALS

Supplementary Tables

Please browse Full Text version to see the data of Supplementary Tables 2 to 3.

Supplementary Table 1. The checklist of quality assessment for the included cortical thickness studies.

12-point checklist

Category 1: Subjects

1. Patients were evaluated prospectively, specific diagnostic criteria were applied, and demographic data were reported.
2. Healthy comparison participants were evaluated prospectively; psychiatric and medical illnesses were excluded.
3. Important variables (e.g., age, gender, drug status, illness duration, motor symptom severity, disease stage, and cognitive function) were checked either via stratification or statistics.
4. Sample size per group: ≥ 20 , scores 1; ≥ 7 , scores 0.5

Category 2: Methods for image acquisition and analysis

5. Magnet strength: 3T, scores 1; 1.5T, scores 0.5
6. Quality control is performed.
7. The imaging technique used was clearly described so that it could be reproduced.
8. Whole brain cortical analysis was automated without a previously defined region.
9. Spatial coordinates were reported in a standard space (e.g., Talairach or MNI coordinates).

Category 3: Results and conclusions

10. Information about the covariates used, such as age and gender in the statistical model were provided.
11. Statistical results were corrected for multiple comparison scores 1, uncorrected scores 0.5.
12. Conclusions were consistent with the results obtained, and the limitations were discussed.

Total score

Supplementary Table 2. Summary of demographic and clinical characteristics of CTh studies included in the meta-analysis.

Supplementary Table 3. Imaging characteristics of the CTh studies included in the meta-analysis.